THREE DIMENSIONAL BOUNDARY LAYERS IN INTERNAL FLOWS

by

R.J. Bodonyi

Prepared under Grant No. NAG 3-528 by the

Indiana University

Research and Sponsered Programs

355 N. Lansing Street

Indianapolis, Indiana 46202

for

NATIONAL AERONAUTICS & SPACE ADMINISTRATION

August 1987.

TABLE OF CONTENTS

PREFACE

The work described in this report was carried out under Grant No. NAG 3-528 "Three-Dimensional Boundary Layers in Internal Flows". The program was monitored by Dr. H.C. Kao, Aerodynamics & Engine Systems Division, NASA Lewis Research Center. The principal investigator was Professor Richard J. Bodonyi, Department of Mathematical Sciences, Indiana University - Purdue University at Indianapolis*. This report constitutes the final technical report for this project.

* Permanent address: The Ohio State University, Department of Aeronautical and Astronautical Engineering, 2036 Neil Ave. Mall, Columbus, Ohio 43210

SUMMARY

A numerical study of the effects of viscous-inviscid interaction in three-dimensional duct flows is presented. In particular we consider interacting flows for which the oncoming flow is not fully-developed. In this case there is a thin boundary layer still present upstream of the of the surface distortion, as opposed to the fully-developed pipe flow situation wherein the flow is viscous across the entire cross section.

1. INTRODUCTION

There exist several reliable methods (e.g. Vatsa & Davis 1973, Blottner 1975, Cebeci, Kaups & Ramsey 1977, McLean & Randall 1979, Lindhout, Moek, Deboer & van der Berg 1979) for calculating standard (or direct) three-dimensional boundary-layer flows with the pressure prescribed. However, such methods are seldom useful in real flows because of the classical separation singularity, among other things. Instead viscous-inviscid interaction generally occurs with both the pressure and the boundary-layer displacement unknown in advance, just as in two-dimensional flows.

Smith (1983) has studied the properties of, and a finite-difference approach for, interactive three-dimensional boundary layers in external flow problems. He found that, contrary to the results of two-dimensional interactions, the three-dimensional inverse problem is an elliptic one and therefore standard foward-marching in the flow direction, e.g. through cross-flow planes, is strictly inappropriate/dangerous because an explosive 3-D free interaction can be initiated. The same phenomena can take place in the interactive case, or whenever the pressure is not described. To overcome these problems, Smith (1983) and Edwards, Carter, & Smith (1987) developed an unconventional finite-difference approach for the external three-dimensional inverse and triple-deck problems which addresses the major numerical difficulties of ellipticity and violent three-dimensional free interactions which are inherent in the standard foward-marching schemes. In this paper the numerical scheme developed by Smith

for three-dimensional interactive flows is generalized to include three-dimensional internal flows with viscous-inviscid interaction, such as in a transition duct. More specifically, we study the interactive flow field present in a duct when the oncoming flow is not yet fully-developed, i.e., in those situations where the entry length isn't long enough for the flow to become fully-developed. In these cases there will still be a "thin" boundary layer on the wall of the duct and hence the possibility of viscous-inviscid interaction in the vicinity of the surface distortion with a nonzero incremental displacement thickness function, $A(x,\theta)$.

2. GOVERNING EQUATIONS

For a developing flow in the geometry shown schematically in Figure 1, it can be shown, following Smith (1976), that the flow structure is three-tiered, consisting of a viscous sublayer I of thickness $O(Re^{-2/5})$, a main deck II of thickness $O(Re^{-1/5})$, which is an inviscid rotational perturbation of the incoming boundary-layer flow, and a potential core region III of thickness $O(1)$, where $Re = a^*U^*/\nu$ is a representative Reynolds number based on the radius a^* of a straight pipe of circular cross section, the centerline velocity U^* in the oncoming flow, and the fluid's kinematic viscosity, ν. Furthermore, we assume that the disturbance (e.g. corner, hump, indentation, etc) size is of the same order of magnitude as the perturbation to the oncoming shear flow. Unlike most problems involving viscous-inviscid interactions, the problem considered here reduces to a consideration of the equations of motion in the viscous sublayer I and the outer core region III. Thus in I we let

$$
\begin{aligned}
&r = 1 - Re^{-2/5},\ Y = O(1),\ X = O(1),\ \theta = O(1)\\
&\tilde{u}(r,\theta,X) = Re^{-1/5}U(Y,\theta,X) + \ldots\ ,\\
&\tilde{v}(r,\theta,X) = Re^{-3/5}V(Y,\theta,X) + \ldots\ ,\\
&\tilde{w}(r,\theta,X) = Re^{-1/5}W(Y,\theta,X) + \ldots\ ,\\
&\tilde{p}(\theta,X) = Re^{-2/5}P(\theta,X) + \ldots\ ,
\end{aligned}
\qquad (2\text{-}1)
$$

where (r,θ,X) are suitably nondimensionalized cylindrical polar coordinates, $(\tilde{v},\tilde{w},\tilde{u})$ the corresponding velocity components and $\tilde{p}$ the nondimensional pressure. Then it is readily shown that in region I the Navier-Stokes equations reduce to the three-dimensional boundary-layer equations, viz:

$$U_X + V_Y + W_\theta = 0 \qquad (2\text{-}2)$$

$$UU_X + VU_Y + WU_\theta = -P_X + U_{YY}, \qquad (2\text{-}3)$$

$$UW_X + VW_Y + WW_\theta = -P_\theta + W_{YY}, \qquad (2\text{-}4)$$

with boundary conditions

$$U = V = W = 0 \text{ on } Y = F(X,\theta), \qquad (2\text{-}5)$$

where $F(X,\theta)$ is a suitably normalized wall shape function such that $F \to 0$ as $X \to -\infty$, and $F(X,\theta+2L) = F(X,\theta)$;

$$U(Y,\theta,X) \to Y,\ V,W,P,A \to 0, \text{ as } X \to -\infty, \qquad (2\text{-}6)$$

and

$$U \sim Y + A(X,\theta),\ Y \to \infty, \text{ all } X, \qquad (2\text{-}7)$$

$$W_X \sim -P_\theta/(Y+A),\ Y \to \infty, \text{ all } X, \qquad (2\text{-}8)$$

and periodicity in θ.

Here (2-5) corresponds to the no-slip condition, (2-6) corresponds to matching with the upstream incident flow, and (2-7) results from a matching of the boundary-layer flow in I to the inviscid rotational flow in region II. The function $-A(X,\theta)$ represents the unknown incremental displacement thickness and is linked to the unknown pressure $P(X,\theta)$ by means of the quasi-inviscid properties in the core flow III.

In the core region we must solve for $P_{inv}(r,\theta,X)$, where

$$\nabla^2 P_{inv} = 0, \qquad (2\text{-}9)$$

along with the boundary conditions

$$P_{inv} = P(X,\theta) \quad @\ r = 1,$$

$$(P_{inv})_r = -A_{XX} \quad @\ r = 1, \qquad (2\text{-}10)$$

regularity at $r = 0$.

Finally, to facilitate the numerical computations the governing equations in the viscous sublayer are rewritten using Prandtl's transposition theorem, viz

$$y = Y - F(X,\theta), \quad x = X,$$

$$v = V - UF_X - WF_\theta, \tag{2-11}$$

$$u(y,\theta,x) = U(Y,\theta,X), \; w(y,\theta,x) = W(Y,\theta,X),$$

$$p(x,\theta) = P(X,\theta).$$

Then equations (2-2) - (2-4) become

$$u_x + v_y + w_\theta = 0, \tag{2-12}$$

$$uu_x + vu_y + wu_\theta = -p_x + u_{yy}, \tag{2-13}$$

$$uw_x + vw_y + ww_\theta = -p_\theta + w_{yy}, \tag{2-14}$$

with boundary conditions

$$u = v = w = 0 \quad \text{on } y = 0, \text{ all } x,\theta, \tag{2-15}$$

$$u \sim y + F(x,\theta) + A(x,\theta), \; y \to \infty, \text{ all } x, \tag{2-16}$$

$$w_x \sim -p_\theta/(y+A+F), \; y \to \infty, \text{ all } x, \tag{2-17}$$

$$u \sim y, \; v,w,p,A \to 0, \quad x \to -\infty, \text{ all } y, \tag{2-18}$$

and periodicity in θ.

As noted by Smith (1976,1980) these equations are elliptic in the pressure field and therefore require a modification of the multi-sweep forward-marching methods developed successfully for two-dimensional flow problems. In the present work the ellipticity embedded in the pressure field needs special attention for otherwise an explosive 3D free interaction can be set off in a forward-marching procedure. Consider the sum of the x-derivative of (2-13), the y-derivative of (2-14) and the x-derivative of (2-12). then defining the skewed shears in the following manner:

$$\bar{u} = u_x + w_\theta, \; \bar{v} = v_x, \tag{2-19}$$

the fundamental governing equations can be written as

$$\bar{u}_x + \bar{v}_\theta = 0, \tag{2-20}$$

$$u\bar{u}_x + u_y\bar{v} = -\bar{\bar{E}} + \bar{u}_{yy} - S \tag{2-21}$$

where

$$S(x,y,\theta) = u_x^2 + vu_{xy} + (wu_\theta)_x + u_\theta w_x + (vw_y)_\theta + (ww_\theta)_\theta, \quad (2\text{-}22)$$

and

$$\bar{\bar{E}} = p_{xx} + p_{\theta\theta}. \quad (2\text{-}23)$$

In these equstions $\bar{u}$, $\bar{v}$, and $\bar{E}$ are treated as the unknowns and the following boundary conditions are applied

$$\bar{u} = \bar{v} = 0 \text{ @ } y = 0, \text{ all } x, \quad (2\text{-}24)$$

$$\bar{u}, \bar{v}, \bar{\bar{E}} \rightarrow 0, -x \rightarrow \infty, \quad (2\text{-}25)$$

$$\bar{u} \sim (A+F)_x, \bar{v}+\bar{\bar{E}} \sim u(A+F)_{xx} - (A_x+F_x)^2, y \rightarrow \infty, \text{ all } x. \quad (2\text{-}26)$$

Note that in these variables the governing equations (2-20) - (2-21) are quasi two-dimensional and linear in the unknown variables.

In the core region, III, we must solve

$$\nabla^2 E = E_{rr} + r^{-1}E_r + r^{-2}E_{\theta\theta} + E_{xx} = 0, \quad (2\text{-}27)$$

where

$$E(x,r,\theta) = p_{xx} + p_{\theta\theta} \quad (2\text{-}28)$$

with

$$\bar{\bar{E}}(x,\theta) = E(x,1,\theta), \quad (2\text{-}29)$$

and

$$E(x,r,\theta) \text{ bounded as } r \rightarrow 0. \quad (2\text{-}30)$$

In the numerical computations we find it convenient to introduce an alternative variable to the displacement function $A(x,\theta)$, namely $B(x,\theta)$, where

$$B(x,\theta) = A_{xx}. \quad (2\text{-}31)$$

The (key) matching relationship is then given by

$$E_r(x,1,\theta) = -(B_{xx} + B_{\theta\theta}). \quad (2\text{-}32)$$

We also find it convenient to rewrite (2-26) somewhat, using

(2-31) together with (2-16), to give

$$\bar{u} \sim \int_{-\infty}^{x} B\,dx + F_x, \tag{2-33}$$

$$\bar{v} + \bar{E} \sim -u(B+F_{xx}) - u_x^2 \tag{2-34}$$

as $y \to \infty$ for all x, θ.

For convenience, symmetry about the plane $\theta = 0$ was taken with reflection conditions $(u,v,w,p)(x,-y,\theta) = (u,v,-w,p)(x,y,\theta)$; to account for periodicity, reflection conditions were also applied at $\theta = L$, for some constant L.

3. NUMERICAL PROCEDURE

The nature of the boundary-layer problem described above suggests an iterative multi-sweep technique, using forward marching in a quasi two-dimensional manner to solve for $\bar{u}$, $\bar{v}$ and E with u, w, and S assumed known from the previous iteration (or an initial guess). Simultaneously, we use standard central differences in order to solve (2-27).

Specifically, given a guess or update for u,v,w and therefore S everywhere, (2-20) - (2-21), (2-24) - (2-26), are marched forward in x, while at the same time (2-27), (2-29), (2-30) are solved along a line of varying r; this then determines $\bar{u},\bar{v},E,E,B$ (and, hence A) along a line of constant spanwise coordinate. The process is then repeated at all other spanwise coordinates. Next the surface pressure $p(x,\theta)$ is found from the Poisson equation (2-33). Updated values of w are found next by marching (2-14) forward in x for each θ, subject to (2-15) - (2-17), assuming that u,v,p and w_θ are known. Finally updated values of u and v are found by an integration of (2-19) with respect to x along with (2-15) and (2-16). All the above steps constitute one global iteration. Convergence is attained when a global convergence test on u is satisfied.

The main features of the numerical scheme are the following. Two and three-point differencing in y is used for (2-20) and (2-21), respectively, with (2-26) applied at $y = y_\infty$, two-point differencing in x and three-point differencing in θ when S is evaluated, at a given x,θ location. This scheme reflects the fact that the flow is generally parabolic in x but elliptic in y.

Three-point central differencing is used to approximate (2-27) in all three dimensions , and (2-32) is approximated by three-point one-sided differencing. Supposing we have n points in y, m points in r, then at each x,θ station the difference approximation of (2-20), (2-21) and (2-27), together with the interface conditions (2-32) - (2-33), may be written schematically in the following form (where an X denotes a non-zero entry and 0 a zero entry):

$$
\begin{bmatrix}
\text{XX00} & & 0 & (2\text{-}20) \\
\text{XXXX} & & \text{X} & (2\text{-}21) \\
\text{XXXX00} & & 0 & (2\text{-}20) \\
\text{XXXXXX} & & \text{X} & (2\text{-}21) \\
\text{XXXX00} & & 0 & (2\text{-}20) \\
\text{XXXXXX} & & \text{X} & (2\text{-}21) \\
\text{XXXX00} & & 0 & (2\text{-}20) \\
\text{XXXXXX} & & \text{X} & (2\text{-}21) \\
 & \cdot & \cdot & \\
 & \cdot & \cdot & \\
 & \cdot & \cdot & \\
(2\text{-}20) & \text{XXXX0000} & & \\
(2\text{-}21) & \text{XXXXXXOX} & & \\
(2\text{-}20) & \text{XXXX00} & & \\
(2\text{-}34) & \text{XOXX} & & \\
(2\text{-}33) & \text{XX0} & & \\
(2\text{-}32) & \text{XXXX} & & \\
(2\text{-}27) & \text{XXX} & & \\
(2\text{-}27) & \text{XXX} \ \ldots & \cdot & \\
 & & \cdot & \\
 & & \cdot & \\
(2\text{-}27) & & \text{XXXO} & \\
(2\text{-}27) & & \text{XX} &
\end{bmatrix}
\begin{bmatrix}
\bar{v}_2 \\ \bar{u}_2 \\ \bar{v}_3 \\ \bar{u}_3 \\ \bar{v}_4 \\ \bar{u}_4 \\ \bar{v}_5 \\ \bar{u}_5 \\ \cdot \\ \cdot \\ \cdot \\ \bar{v}_n \\ \bar{u}_n \\ \bar{B} \\ \bar{E}=E_1 \\ E_2 \\ E_3 \\ E_4 \\ \cdot \\ \cdot \\ \cdot \\ E_{m-2} \\ E_{m-1}
\end{bmatrix}
= \bar{R} \qquad (3\text{-}1)
$$

Here equation numbers denote the equation which the row approximates. Notice that

$$\bar{v}_1 = \bar{u}_1 = 0 \ , \quad E_m = 0 \ . \qquad (3\text{-}2)$$

The solitary column of entries in the upper part of the matrix corresponds to the $\bar{E}$ term in (2-21). (3-1) is then amenable to standard Gaussian elimination procedures. (2-33), which determines the surface pressure, was also approximated by central

differences, and was solved by Gauss-Seidel sweeps (without pivoting), with an over-relaxation parameter until a prescribed tolerance is met. The solution for w is similar to that for $\bar{u}$ and $\bar{v}$ except that only a tri-diagonal matrix requires inversion (performed again using Gaussian elimination). Finally the x-integrations to compute u and v were performed using the trapezoidal rule. The overall scheme is nominally second-order accurate in the mesh widths Δx, Δy, $\Delta\theta$, and Δr.

A crucial feature of the scheme developed as parrt of this research effort is the inherent coupling between the viscous boundary-layer solution and the inviscid core solution which is carried out simultaneously in the spirit of the scheme proposed by Veldman (1979) in treating two-dimensional incompressible flows, using the Hilbert integral approach. This approach has also recently been used by Bodonyi & Duck (1987) to succesfully treat three-dimensional external interacting flows.

4. RESULTS

The numerical method discussed in the previous section has been applied to several test problems. The model problem corresponds to that of a nonfully-developed flow upstream of the surface distortion given by a bounded transition duct with $F(x,\theta)$ defined by

$$F(x,\theta) = \begin{cases} hx^3(1 + x^3)^{-1}\cos(2\theta), & x > 0, \\ 0, & x < 0. \end{cases} \qquad (4-1)$$

and h ranging between 0.6 and 3.2.

In this case the duct undergoes a transition from that of a circular cross section duct far upstream to that of an elliptical cross section far downstream, as shown schematically in Figure 2.

Solutions for the fully developed flow problem upstream of the surface distortion wherein $A(x,\theta) = 0$ have also been found for the same duct shape. ince the solutions for both of these problems are qualitatively similar, only the results for the interactive case are given here. Figures 3 -7 give the axial and azimuthal skin friction distributions and the wall pressure distribution along the line of symmetry for several values of h. No flow reversal was encountered in the axial direction for values of h considered in this report, although the azimuthal skin friction w_y does exhibit a reversal of sign sufficiently far downstream for $h > 1$. All efforts to extend the computations to larger values of h such that axial flow reversal occured were unsuccessful. The difficulties in obtaining solutions for $h > 3.2$ are apparent in the pressure distribution shown in Figure 7. A possible reason for this is that the governing equations are

treated in a quasi-two-dimensional forward marching manner which may not properly account for the transverse velocity component when it becomes sufficiently large as in the bounded transition duct when $h > 3.2$. Unfortunately, within the time frame of this research effort this difficulty was not resolved.

A numerical study of noncircular incident ducts has also been considered. In this case the incident skin friction depends on θ, e.g. parallel flow through an ellipse. The governing equations are the same as before except that now the outer boundary condition (2-16) is replaced by

$$u \sim \lambda(\theta)\{y + A(x,\theta) + F(x,\theta)\}. \qquad (4-2)$$

Here the parameter $\lambda(\theta)$ gives the azimuthal distribution of the incoming shear flow in the viscous sublayer $u = \lambda(\theta)y$.

The numerical scheme discussed above has been adapted to include this effect and representative results for the skin friction distributions when $A(x,\theta) = 0$ and $F(x,\theta)$is given by (4-1) are shown in Figure 8 for $h = 2$ and $\lambda(\theta) = 0.25 + \sin^2\theta$.

Finally, as part of this research effort similarity solutions for $x \rightarrow \infty$ of equations (2-12) - (2-18) for an "unbounded" transition body shape of the form

$$F(x,\theta) \sim x^{1/3}\cos(2\theta) \qquad (4-3)$$

have been investigated with the goal of gaining a better understanding of the flow structure far downstream in the duct. By expanding in powers of θ, the governing equations can be reduced to a set of ordinary differential equations, but in the process several undetermined parameters are introduced. It was found that the appropriate similarity equations permit multiple solutions, as well as regions in parameter space where no

solutions could be found depending on the range of values of the parameters mentioned above. For further details concerning these similarity equations, the interested reader is referred to Bennett (1986) who studied these similarity equations in another context.

REFERENCES

Bennett, J., Ph.D Dissertation, University College London, Department of Mathematics (1986).

Blottner, F.G., AGARD Lecture Series No. 73, Von Karman Institute, 1975.

Bodonyi, R.J. & Duck, P.W., Computers & Fluids, to appear

Cebeci, T., Kaups, K. & Ramsay, J.L., NASA Contractor Report CR-2777, 1977.

Edwards, D.E., Carter, J.E. & Smith, F.T., AIAA J. 25, 380 (1987).

Lindhout, J.P.F., Moek, G. Deboer, E. * van den Berg, B., NLR-MP-79003-U, The Netherlands, 1979.

McLean, J.D. & Randall, J.L., NASA Contractor Report CR-3123., 1979.

Smith, F.T., Mathematika 23, 62 (1976).

Smith, F.T., J. Fluid Mech. 99, 185 (1980).

Smith, F.T., UTRC Report 83-46, United Technologies Research Center, (1983).

Vatsa, V.N. & Davis, R.T., NASA Contractor Report CR-112315, 1973.

Veldman, A.E.P., NLR-TR-79023, Netherlands Nat. Aerosp. Lab. (1979).

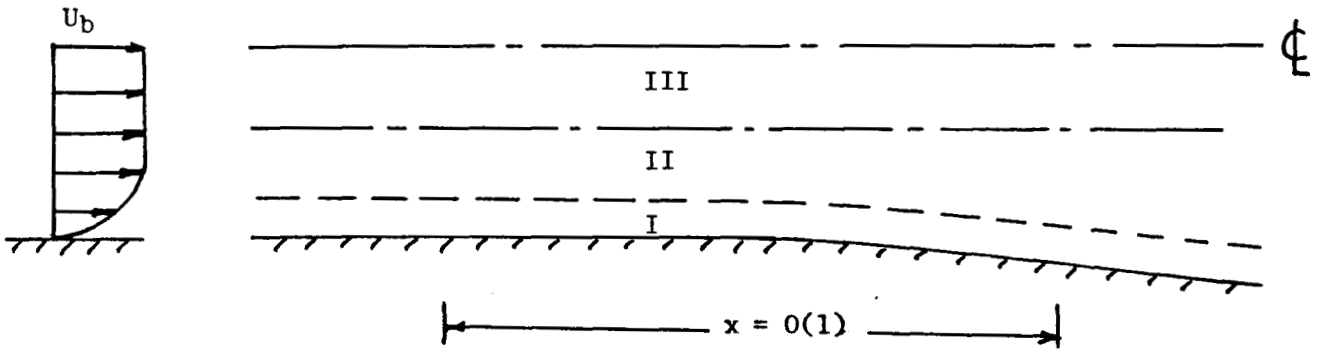

Figure 1. Schematic of the Flow Field Geometry.

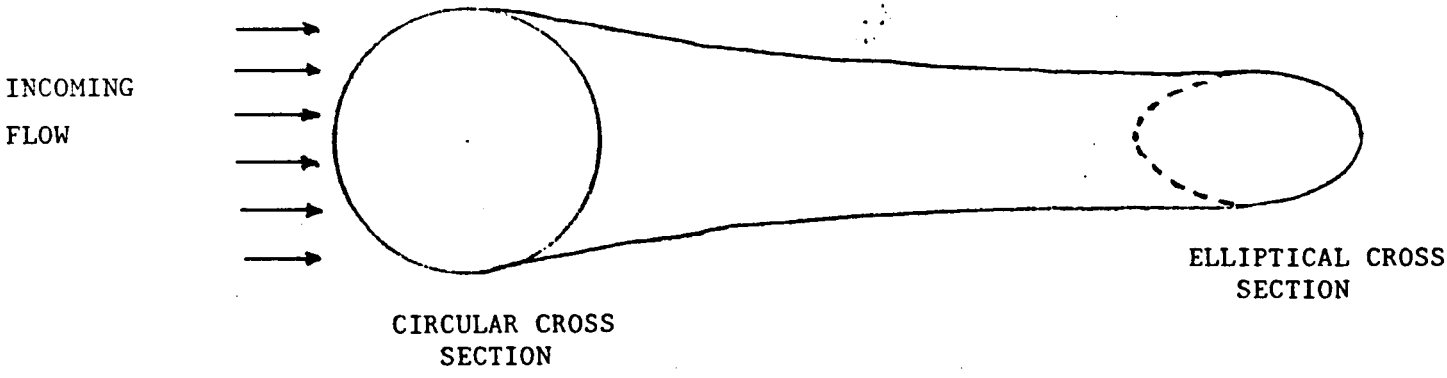

Figure 2. Schematic of Duct Geometry for Bounded Transition Flow Given by Equation 36.

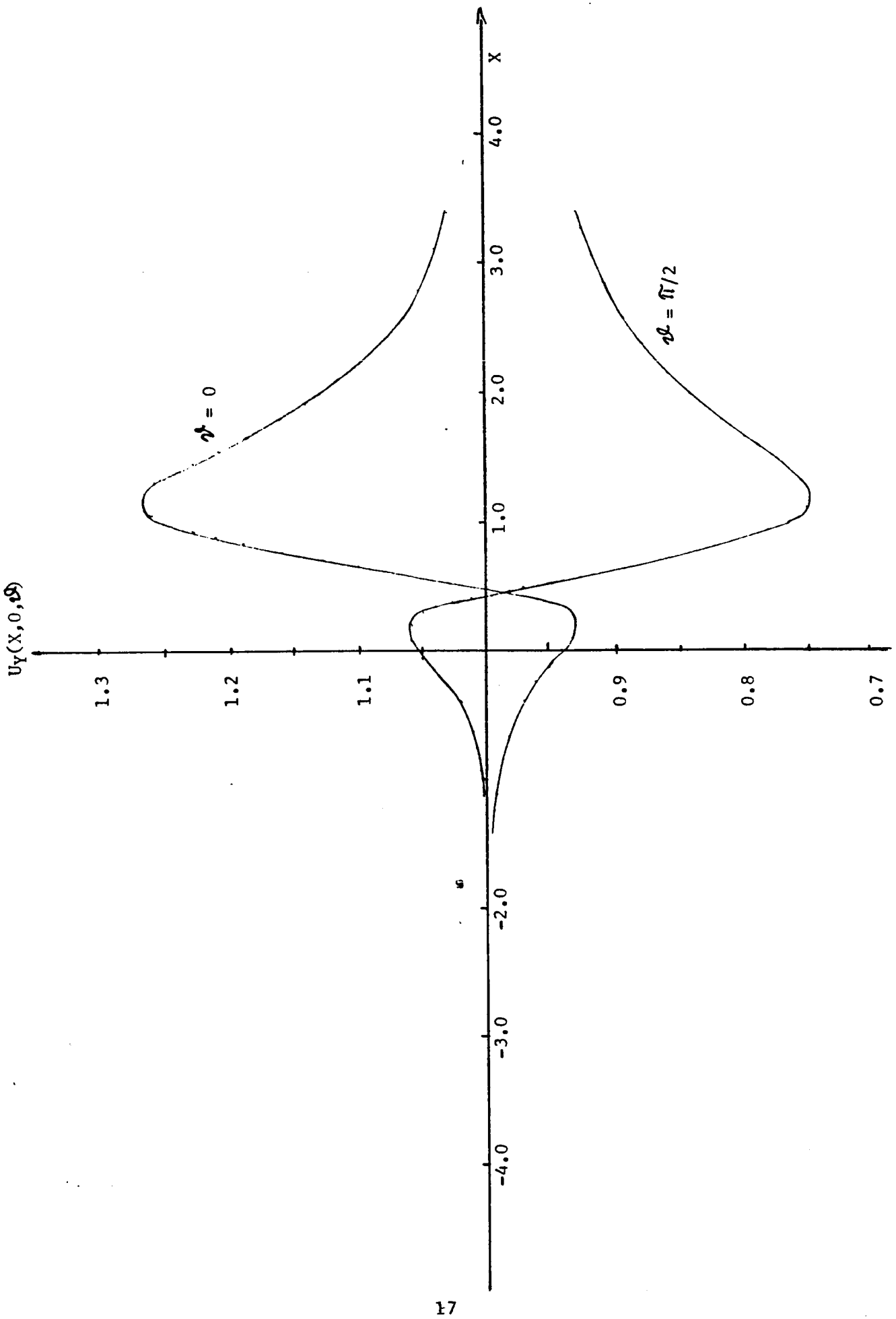

Figure 3. Axial Wall Shear Stress for a Bounded Transition Duct, h = 1.0

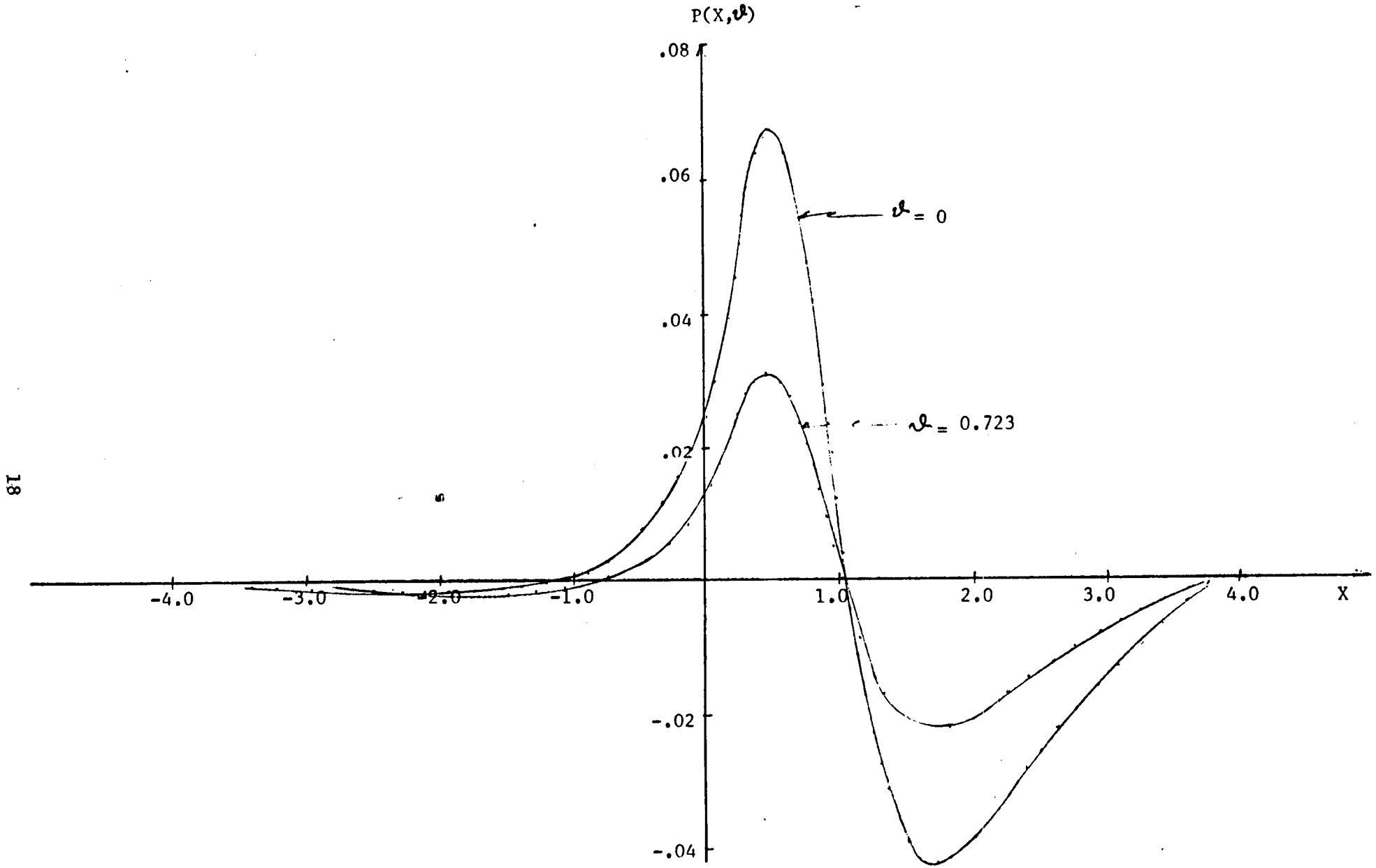

Figure 4. Pressure Distribution for a Bounded Transition Duct, h = 1.0

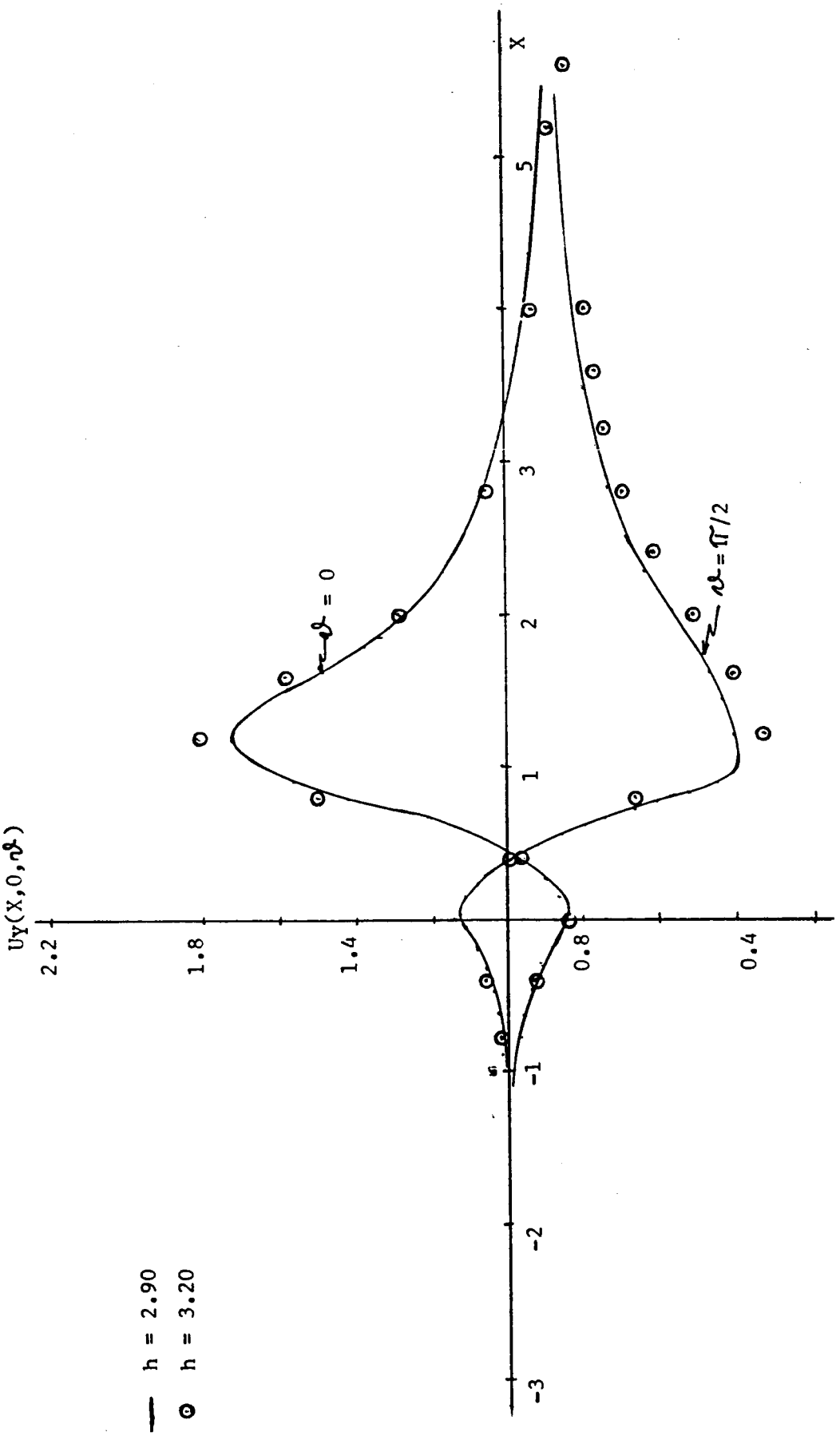

Figure 5. Axial Wall Shear Stress for a Bounded Transition Duct.

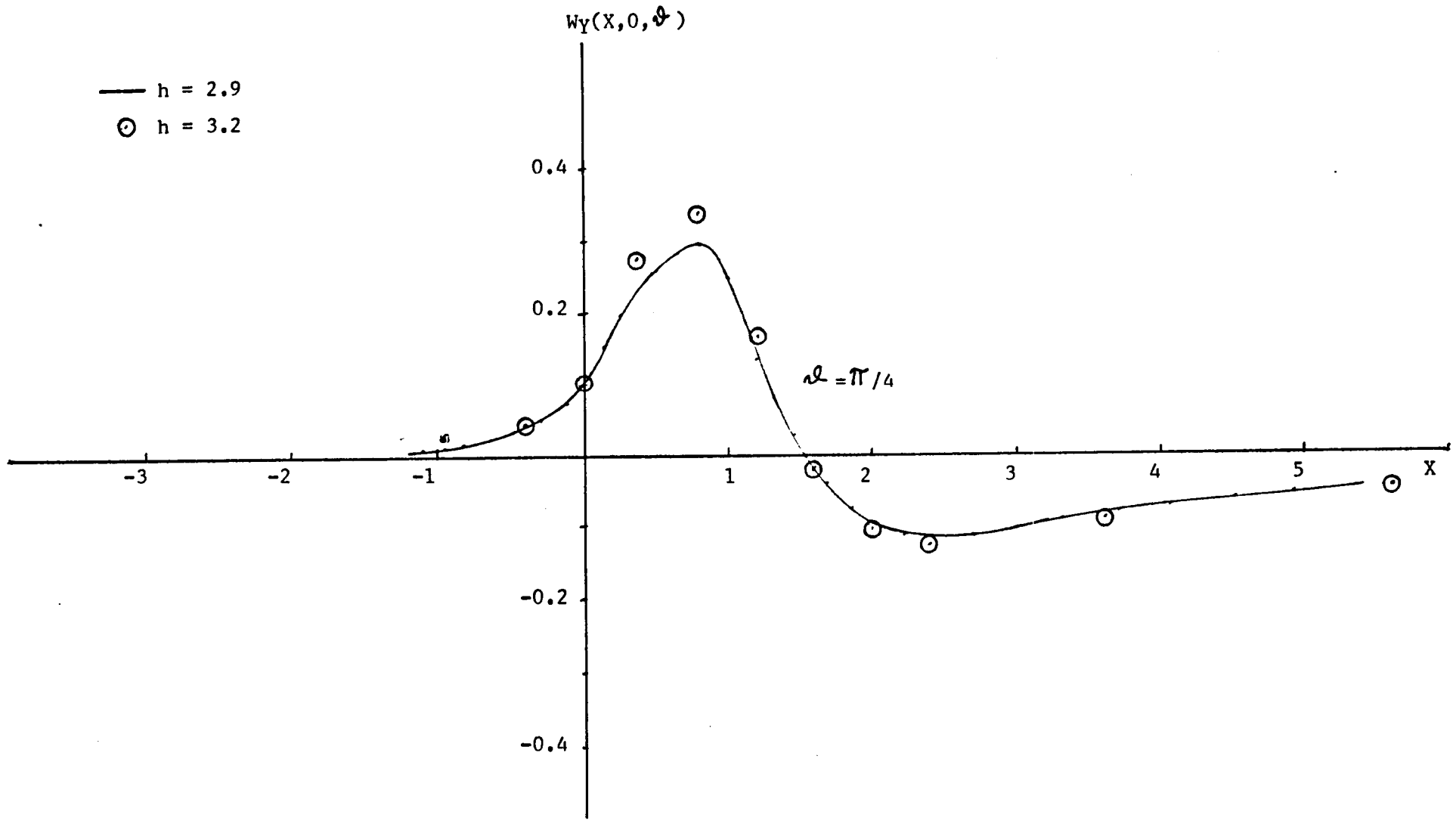

Figure 6. Azimuthal Wall Shear Stress for a Bounded Transition Duct.

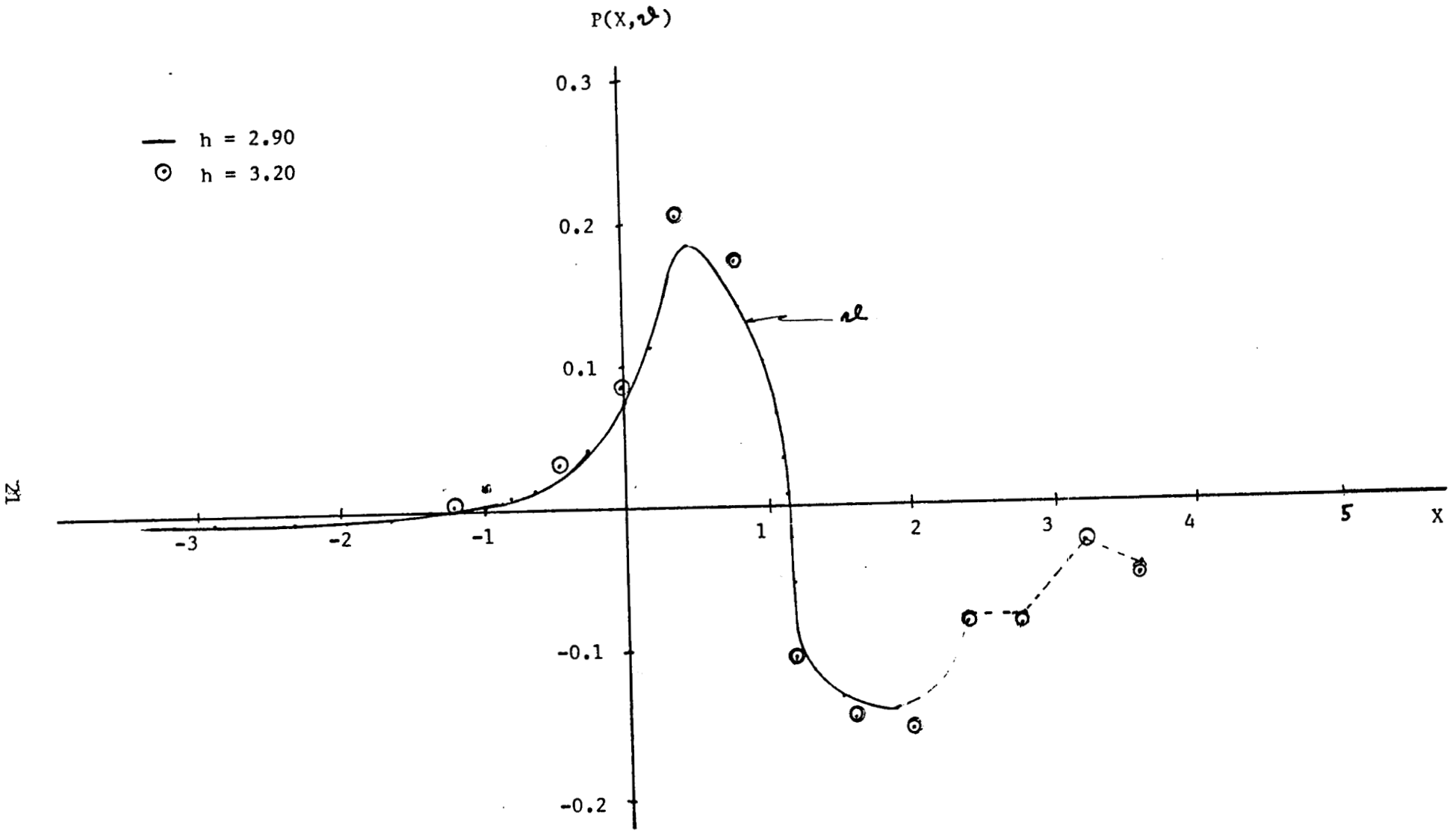

Figure 7. Pressure Distribution for a Bounded Transition Duct.

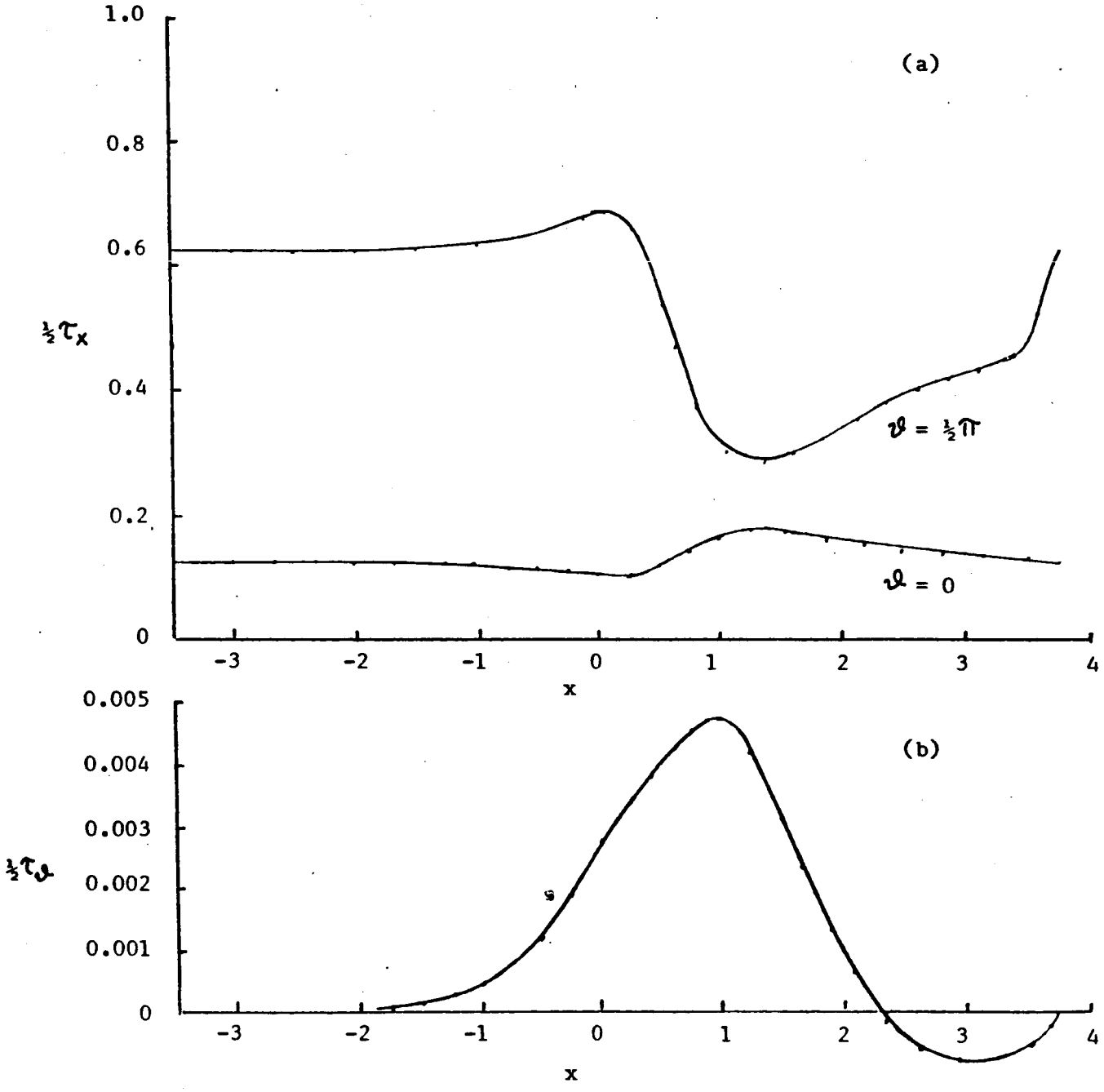

Figure 8. (a) Axial and (b) azimuthal skin friction distributions for a variable incident skin friction duct flow.